Received: 24 July 2023 | Accepted: 4 August 2023
DOI: 10.1111/1462-2920.16504

RESEARCH ARTICLE

ENVIRONMENTAL MICROBIOLOGY
Applied Microbiology International

Geochemical factors impacting nitrifying communities in sandy sediments

Stephanie J. Wilson[1,2] | **Bongkeun Song**[1] | **Iris C. Anderson**[1]

[1]Department of Biological Sciences, Virginia Institute of Marine Science, College of William & Mary, Gloucester Point, Virginia, USA
[2]Smithsonian Environmental Research Center, Edgewater, Maryland, USA

Correspondence
Stephanie J. Wilson, Smithsonian Environmental Research Center, Edgewater, MD, USA.
Email: wilsonsj@si.edu

Funding information
National Science Foundation, Grant/Award Numbers: 1658135, 1737258

Abstract

Sandy sediment beaches covering 70% of non-ice-covered coastlines are important ecosystems for nutrient cycling along the land-ocean continuum. Subterranean estuaries (STEs), where groundwater and seawater meet, are hotspots for biogeochemical cycling within sandy beaches. The STE microbial community facilitates biogeochemical reactions, determining the fate of nutrients, including nitrogen (N), supplied by groundwater. Nitrification influences the fate of N, oxidising reduced dissolved inorganic nitrogen (DIN), making it available for N removal. We used metabarcoding of 16S rRNA genes and quantitative PCR (qPCR) of ammonia monooxygenase (*amoA*) genes to characterise spatial and temporal variation in STE microbial community structure and nitrifying organisms. We examined nitrifier diversity, distribution and abundance to determine how geochemical measurements influenced their distribution in STEs. Sediment microbial communities varied with depth (p-value $= 0.001$) and followed geochemical gradients in dissolved oxygen (DO), salinity, pH, dissolved inorganic carbon and DIN. Genetic potential for nitrification in the STE was evidenced by qPCR quantification of *amoA* genes. Ammonia oxidiser abundance was best explained by DIN, DO and pH. Our results suggest that geochemical gradients are tightly linked to STE community composition and nitrifier abundance, which are important to determine the fate and transport of groundwater-derived nutrients to coastal waters.

INTRODUCTION

Sandy beaches cover roughly 70% of coastlines without ice (McLachlan & Brown, 2006). These coastal systems are important habitats that influence and regulate the cycling of nutrients, carbon and trace metals (Anschutz et al., 2016; Beck et al., 2017; Santoro, 2010; Santos et al., 2008). Within the subsurface of sandy beaches, fresh groundwater flow meets and mixes with intruding seawater in the subterranean estuary (STE; Moore, 1999), an important transition zone along the land-ocean continuum.

The mixing of these two distinct water bodies in STEs is facilitated by the high hydraulic conductivity often observed in sandy, permeable sediments resulting in highly variable systems. Steep geochemical gradients are characteristic of STEs, which often act as biogeochemical hotspots for nutrient, trace metal and organic matter cycling. Microbial communities facilitate biogeochemical processes in the subsurface such as respiration, sulphate reduction, iron oxidation or reduction, methanogenesis, nitrogen cycling pathways and many others (Hong et al., 2019; Hug et al., 2016; Wu et al., 2021). Transformations mediated by microbial communities along the STE flow path determine the concentration and speciation of nutrients, such as nitrogen (N), and other analytes that are discharged to the overlying water by submarine groundwater discharge (SGD) and porewater exchange (Beck et al., 2016; Couturier et al., 2017; Ruiz-González et al., 2021; Santoro, 2010; Santos et al., 2008; Slomp and Van Capellen, 2004; Wu et al., 2021). STE microbial communities have been observed to vary with temperature, salinity, pH, redox conditions and nutrient concentrations

© 2023 Applied Microbiology International and John Wiley Sons & Ltd.

(Ruiz-González et al., 2021 and citations therein). Despite their role in determining nutrient fluxes, many of the transformations that occur in sandy beaches and the microbial communities that support them remain poorly characterised.

Groundwater can accumulate considerable amounts of dissolved inorganic nitrogen (DIN) along its flow path. Reduced DIN in groundwater, such as ammonium (NH_4^+) may be oxidised by nitrification to nitrite (NO_2^-) and then to nitrate (NO_3^-) in the STE. Nitrification is an important process as it makes oxidised forms of DIN available for conversion to dinitrogen gas (N_2) by the microbial N removal processes: denitrification and anaerobic ammonium oxidation (anammox). In STEs with high groundwater NH_4^+ concentrations, nitrification is required for N removal and subsequently determines DIN concentrations in SGD. Coupled nitrification–denitrification has been shown to remove up to 50% of external DIN inputs to estuaries (Seitzinger et al., 2006). Erler et al. (2014) observed that 80% of observed NH_4^+ in a tropical STE was consumed by nitrification making it available for denitrification. In addition, the product of nitrification (NO_3^-) is more mobile than the reactant (NH_4^+) and is more easily discharged, which may result in higher DIN discharge via SGD.

Nitrification occurs in two steps: ammonia oxidation and nitrite oxidation. Ammonia oxidation, which oxidises NH_4^+ to NO_2^-, is the rate-limiting step mediated by ammonia oxidising archaea (AOA) and ammonia oxidising bacteria (AOB). Ammonia monooxygenase, encoded by *amo* genes, catalyses ammonia oxidation. The second step of nitrification, nitrite oxidation, is the oxidation of NO_2^- to NO_3^- and is mediated by nitrite oxidoreductase encoded by *nxr* genes in nitrite oxidising bacteria (NOB). Complete ammonia oxidisers (comammox) can conduct both steps of nitrification (Santoro, 2016; van Kessel et al., 2015).

The *amoA* gene is often used as a genetic marker for studying nitrification in the environment and has been observed in estuaries (Caffrey et al., 2007; Lisa et al., 2015), groundwater (Reed et al., 2010) and STEs (Hong et al., 2019; Santoro et al., 2008). Nitrifier abundance and community composition have been related to salinity (Cardarelli et al., 2020; Prosser & Nicol, 2008; Santoro, 2010; Santoro et al., 2008) and dissolved oxygen (DO) concentrations (Santoro, 2010). Despite previous work, it remains unclear what influences shifts in the composition and abundance of nitrifying communities within STEs. Steep geochemical gradients often observed in STEs, and their dynamic nature, provide an ideal system to investigate geochemical factors affecting community structure and abundance in coastal systems.

This study examined how sediment microbial communities vary with depth and season in a STE, with a focus on nitrifying communities. Four objectives for this study include (1) to examine sediment microbial community composition along geochemical gradients, (2) to identify bacterial and archaeal taxa of nitrifying communities (AOA, AOB and NOB), (3) to quantify AOA and AOB abundances and (4) to determine geochemical features influencing AOA and AOB distributions. Sediment microbial communities were examined with depth during four seasons at the Gloucester Point STE (GP-STE), a well-studied STE at a sandy sediment beach along the York River Estuary, a tributary of the Chesapeake Bay (Beck et al., 2016, Hong et al., 2019, Wilson et al., 2023). In the spring, summer, fall and winter (2018–2019), porewater and one 110 cm-long core were collected (*Methods*). We used a molecular approach combining a metabarcoding analysis of 16S rRNA genes to examine microbial community composition and qPCR of *amoA* genes to determine spatial and temporal variation in AOA and AOB abundances in STE sediments, followed by statistical analyses to elucidate important geochemical features influencing resident nitrifying communities.

EXPERIMENTAL PROCEDURES

Sampling site and sample collection

Samples were collected at a STE located at the Gloucester Point Beach (GP-STE: 37.248884° N, 76.505324° W), VA, USA. The beach is a part of the lower York River Estuary (YRE), a microtidal tributary (tidal range ~0.7–0.8 m) of the Chesapeake Bay. This is a sandy sediment beach with a man-made jetty on either side; a detailed site description can be found in Beck et al. (2016).

Porewater and sediment were sampled four times, in April, July and October of 2018 and January of 2019, referred to here as spring, summer, fall and winter, respectively. Sediment samples were obtained with a vibracore with the resulting four cores ranging from 120 to 260 cm in length; however, only the top 110 cm was used in this study. After transport to the lab, sediment cores were sectioned into 10 cm increments and homogenised (47 total samples). A subsample from each core section was frozen at −80°C for DNA extraction and another subsample was stored at 4°C for sediment characterisation and nutrient extraction. To collect extractable nutrients, 1 M potassium chloride (KCl) was added to 4 g of sediment, shaken for 1 h before decanting and filtering the extract with a 0.45 μm Whatman Puradisc membrane filter (GE Healthcare Life Sciences). Extracted samples were analysed for inorganic nutrients NO_3^-, NO_2^- and NH_4^+ on a Lachat QuikChem 8000 automated ion analyzer (Lachat Instruments, Milwaukee, WI, USA).

Porewater samples were obtained from dedicated piezometers with 2 cm screens (AMS Gas Vapour Tip) attached to Fluorinated Ethylene Propylene (FEP) tubing (VersilOn, Saint-Gobain), positioned at 10 cm increments from the sediment surface to 120 cm (Charette et al., 2006). Masterflex C-Flex L/S Precision Pump tubing (Cole-Palmer) was attached to piezometer tubing and porewater was slowly pumped from the ground with an Alexis V3.0 peristaltic pump (Proactive Environmental Products). Porewater was analysed for salinity, dissolved oxygen (DO) and pH using a flow through YSI (600 XL sonde) or HACH probe (HQ40d meter, Loveland, CO, USA). Nutrient samples were filtered using a 0.45 μM cartridge filter (Millipore Ltd.) and frozen until analysis. Concentrations of porewater NO_3^-, NO_2^- and NH_4^+ were determined on a Lachat QuikChem 8000 automated ion analyzer (Lachat Instruments, Milwaukee, WI, USA).

Molecular analyses: Metabarcoding analysis of 16S rRNA genes

Sediment DNA was extracted from the homogenised 10 cm vibracore subsections using the PowerSoil PowerLyzer kit (Qiagen) following manufacturer instructions. To maximise DNA yield, two bead tubes were used per sample, both filled with 0.5 grams of sediment, replicate products were combined during the spin filter step. DNA was quantified with a Qubit™ fluorometer (Invitrogen) and frozen for later use.

The variable V4 region of the 16S rRNA gene was amplified with a unique barcoded 515FY primer for each sample and a common 806R primer (Caporaso et al., 2012; Parada et al., 2015) following the Earth Microbiome project protocol (Thompson et al., 2017). The PCR mixture for 16S amplification consisted of 12.5 μL of 10× GoTaq Master Mix, 1 μL of each primer (10 nM), 6 μL of nuclease free water and 6 μL of sample DNA (diluted to 0.5 ng/μL). The PCR cycle began with 3 min at 95°C, followed by 25 cycles of 30 s at 95°C, 1 min at 55°C and 1 min at 72°C, followed by 5 min at 72°C. Amplification was confirmed and the negative control assessed using 1% agarose gel electrophoresis (target fragment size 354 bp). Samples were pooled, purified using the Promega Wizard™ SV Gel and PCR Cleanup System, and then sequenced on the MiSeq Platform (Illumina) following the manufacturer's instructions.

Bioinformatic analysis was conducted in R Studio (version 3.2.2. Copyright 2015 The R Foundation for Statistical Computing) using the DADA2 bioinformatic package (Callahan et al., 2016). Primer sequences were trimmed, and raw reads were filtered; only sequences with quality scores >30 were utilised. Samples were denoised and amplicon sequence variants (ASVs) were identified prior to taxonomic classification with the SILVA v138 taxonomy database (Quast et al., 2013). β-diversity was estimated with the Bray–Curtis dissimilarity calculator in the phyloseq package (McMurdie & Holmes, 2013). Nitrifying organisms were identified by manually searching for specific, known genera of AOA, AOB and NOB including: '*Nitrospirota*', '*Nitrospinota*', '*Nitrospira*', '*Nitrospina*', '*Nitrosomonas*', '*Nitrococcus*', '*Nitrosococcales*', '*Nitrobacter*', '*Nitrososphaera*', '*Nitrosopumilus*', '*Nitrososphaerota*' (formerly *Thaumarchaeota*) and '*Nitrososphaeria*'.

Molecular analyses: *amoA* gene qPCR assays

The abundance of *amoA* genes from AOA and AOB were determined by qPCR assays with a QuantStudio 6 Flex (Thermo Scientific) using primer pairs *amoA*F and *amoA*R (Francis et al., 2005) and amoA1F and amoA2R (Rotthauwe et al., 1997), respectively. It should be noted that the *amoA*-1F and *amoA*-2R primer pair only amplifies β-proteobacteria. Standards were prepared by serial dilution of plasmids carrying target *amoA* genes obtained from environmental samples. The standards were quantified using an Agilent 220 TapeStation System (Agilent Technologies) following a digestion with ECoR1 (Lisa et al., 2015). Archaeal and bacteria *amoA* gene assays were conducted in triplicate on 384 well plates and included negative controls with no DNA template. Each reaction had a total volume of 12 μL consisting of 6 μL 1× SYBR green GoTaq qPCR Master Mix (Promega), 0.12 μL bovine serum albumin (1 nM), 1 μL of each primer (6 μM), 0.05 μL CRX dye, 4 μL sample DNA (diluted to a concentration of 0.5 ng/μL) and adjusted to the final volume with nuclease-free water. The qPCR conditions for both AOA and AOB *amoA* gene began with 10 min at 95°C, followed by 45 cycles of 15 s at 95°C, 45 s at 53°C, 30 s at 72°C and 35 s at 80°C (data acquisition). This was followed by dissociation step consisting of 15 s at 95°C, 1 min at 60°C, 15 s at 95°C and finally 19 s at 60°C (Lisa et al., 2015; Wu et al., 2021). The efficiency and R^2 values for the AOA *amoA* standard curve were 78% and 0.99, respectively; the efficiency and R^2 values for the AOB *amoA* gene standard curve were 98% and 0.99, respectively. The limit of detection (LOD) for each assay was set as the concentration of the lowest standard of the standard curve any samples below this quantity were considered below detection (bdl). The LODs were 185 and 74 copies per reaction before normalisation for DNA concentration for the *amoA* AOA and *Betaproteobacterial* AOB assays, respectively. The determined quantities of *amoA* were normalised to the number of copies of the *amoA* found in a single AOA (Qin et al., 2016; Tourna et al., 2011) or AOB organism (Norton et al., 2002; Okano et al., 2004). It should be noted that *amoA* genes from comammox were also tested for in all samples using primer sets *comaA* and *comaB* but were not detected in the GP-STE (Pjevac et al., 2017).

Statistical analyses

All statistical analyses were conducted in R studio (The R Foundation for Statistical Computing, version 3.2.2. Copyright 2015). The β-diversity of the microbial community in the STE was evaluated with a principal coordinate analysis (PCoA). A permutational multivariate ANOVA (PERMANOVA) using the Adonis function in the vegan package in R (Oksanaen et al., 2019) was used to assess the fixed effects of season and depth on microbial community composition. We also used a constrained ordination (CAP) analysis in which ordination axes are constrained to linear combinations of environmental variables. This allows us to examine how environmental variables are associated with changes in community composition. Porewater geochemical variables were included in the CAP analysis. A permutational ANOVA on the constrained axes used in ordination (distance $\sim$ Salinity $+$ NO3 $+$ NH4 $+$ DO $+$ DIC $+$ pH; p-value $= 0.001$) was used to determine the statistical significance of the model.

A one-way ANOVA was used to assess the effect of season on qPCR *amoA* gene abundances. The *amoA* gene abundances derived from qPCR were then analysed with multiple linear regression models. In the case of abundances being below the detection limit, half of the detection limit was assigned to that depth. AOA and AOB relative abundances based on 16S sequences were positively correlated to qPCR quantification of *amoA* genes in AOA and *Betaproteobacterial* AOB (Figure S6). Co-linearity was assessed using the VIF function in the car package (Fox et al., 2019) in R. The most parsimonious model was determined by Akaike information criterion (dAICc; (Graham et al., 2016), model weights, and variance explained (R^2). dAICc was utilised for model selection to account for limited sample size. Homogeneity of variance and normality were assessed. The data were log-normally distributed, so log-transformed qPCR gene abundances were used in all multiple linear regression models to meet the assumption of normality. All statistical tests were assessed for significance with $\alpha = 0.05$.

RESULTS

Porewater & sediment geochemical parameters

Geochemical gradients in the GP-STE were assessed using porewater profiles collected from dedicated piezometers in each season sampled (48 samples, *Methods*). These profiles are discussed in detail in Wilson et al. (2023). Briefly, the GP-STE was generally characterised by three zones: a surficial and oxic zone from 0 to 50 cm, a suboxic transition zone from 60 to 70 cm, and an anoxic zone below 80 cm (Figure 1). Salinity, DO, and pH decreased as depth increased. Salinity ranged from 3.21 to 18.68, dissolved oxygen (DO) ranged from 0 to 13.2 mg/L, and pH from 7.8 to 8.1 (Figure 1A,B). Porewater DIC concentrations increased with depth, ranging from 1.15 to 6.09 mM (Figure 1A). Porewater NH_4^+, NO_3^- and NO_2^- concentrations ranged from 0.25 to 99.56 μM, 0.02 to 77.61 μM and 0 to 0.5 μM, respectively (Figure 1C). Porewater NH_4^+ increased with depth, whereas NO_3^- concentrations exhibited a peak between 50 and 100 cm, the only region where NO_3^- exceeded 10 μM. NO_2^- concentrations remained constant with depth. Extractable NH_4^+ concentrations, determined for each sediment sample, increased with sediment depth, whereas extractable NO_3^- and NO_2^- remained constant throughout the profiles (Figure 1D). Extractable NH_4^+, NO_3^- and NO_2^- concentrations ranged from 0.53 to 23.93 μM, 2.51 to 6.60 μM and 0 to 1.20 μM respectively.

Microbial community composition

Four cores (110 cm long) collected from the GP-STE, one per season, were sectioned into 10 cm increments resulting in 47 samples (*Methods*). 16S metabarcoding analysis of these samples generated a total of 713,272 reads, with an average of 17,798 reads per sample. As shown in Figure 2, the beta-diversity of the sediment microbial communities varied significantly with depth (p-value $= 0.001$). The STE sediment communities can be differentiated with depth including oxic sediment communities (0–50 cm), suboxic zone communities (60–70 cm) and anoxic sediment communities (80–110 cm). The steep geochemical gradients in the STE were hypothesised to drive this depth zonation and a CAP analysis revealed that porewater DO, nutrients, salinity and DIC explained 21% of the variation observed in the microbial community structure (Figure S2).

The STE microbial community was relatively stable across seasons with no statistically significant effect of season observed (p-value >0.05). Although not statistically significant, some small shifts in microbial community structure with the season are observed. The presence of several families including *Calditrichaceae*, *Desulfarculaceae*, *Desulfobacteraceae* and *Rhodobacteraceae* shift along the STE sediment profile across seasons (Figure 3). *Calditrichaceae* is observed in the top 40 cm of the STE and had higher abundances in spring and winter, than in summer and fall. *Desulfarculaceae* shift to deeper sediments in the fall and winter as compared to spring and summer whereas *Rhodobacteraceae* shift deeper (to 40 cm) in spring and fall and are shallower in summer and winter (0–20 cm). In contrast, *Woeseiaceae* are present in the top 50–60 cm of the STE year-round. Similarly, *Nitrosopumilaceae* is present in the top 0 to 40–50 cm in all seasons.

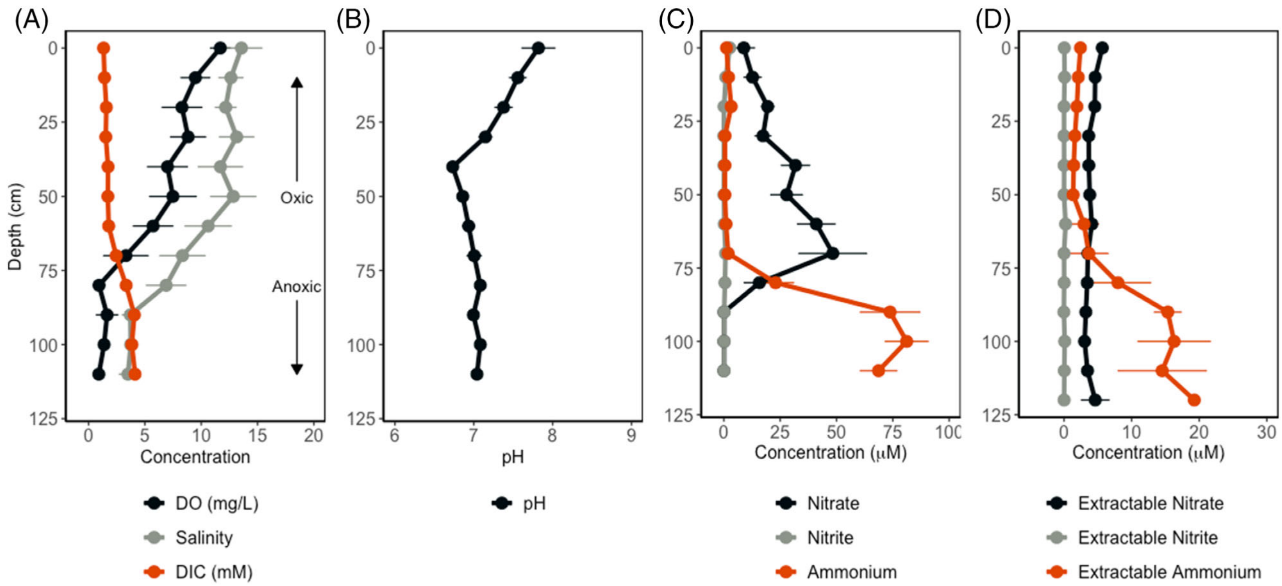

FIGURE 1 GP-STE geochemical depth profiles shown as averages of seasonal measurements. (A) Dissolved oxygen (DO, mg/L), salinity and dissolved inorganic carbon (DIC, mM). (B) pH, (C) nitrate (μM), nitrite (μM) and ammonium (μM). (D) Extractable nitrate (μM), extractable nitrite (μM) and extractable ammonium (μM). Error bars indicate one standard error in each direction.

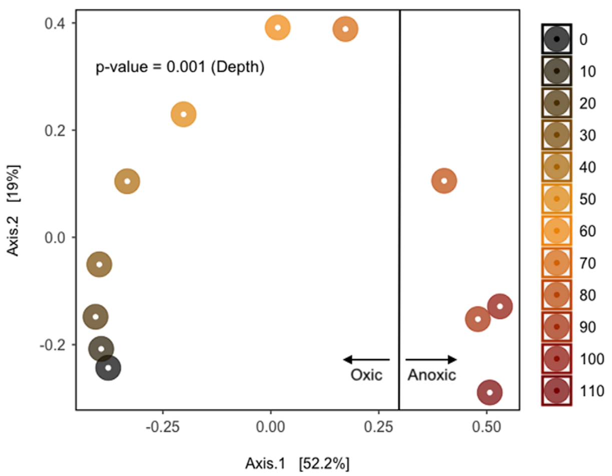

FIGURE 2 Principal coordinate analysis (PCoA) showing microbial community structure merged across seasons at each STE sediment depth (indicated by colour). Depth is labelled with the top depth of the respective core section, for example 0 indicates core section 0–10 cm. Sample dissimilarity was calculated using the Bray–Curtis dissimilarity index and a multivariate permutational analysis of variance (PERMANOVA) was used to analyse amplicon sequence variant (ASV) dissimilarity with depth (p-value <0.001). Figure S2 shows a PCoA with all replicate samples across seasons (p-value >0.05).

The 16S sequences, when combined across seasons and depths, were dominated by bacteria, which represented ~80% of the total identified sequences, while archaea accounted for ~20%. The relative abundance of archaea increased with depth, ranging from 2.0% to 14% at 0 cm and increasing to 30% to 48% at 110 cm. Phyla with the highest relative abundances in the oxic zone of STE sediments included *Acidobacteria*, *Proteobacteria*, *Planctomycetes* and *Bacteriodetes* (Figure S1). In the suboxic and anoxic zones, the most abundant phyla included *Acidobacteria*, *Chloroflexi* and *Planctomycetes* (Figure S1). At the family level, consistent shifts in community composition were observed with depth (Figure 3). For example, *Pirellulaceae*, *Nitrosopumilaceae* and *Methyloligellaceae* are consistently present above 60 cm, whereas *Acidiferrobacteraceae* and *Syntrophaceae* are only observed in sediment samples deeper than 80 cm (Figure 3).

Nitrifiers, including AOA, AOB and NOB taxa, were identified from sediment microbial communities (Figure 4). The relative abundance of AOA sequences ranged from 0.0% to 10.8%, with the majority of AOA present from 0 to 70 cm (Table S1). Two AOA families were identified; *Nitrosopumilaceae* and *Nitrososphaeraceae* (Figure 4). The AOA community was heavily dominated by *Nitrosopumilaceae*, representing >99% of the AOA. The relative abundance of AOB in the GP-STE ranged from 0% to 6.2%, with the highest abundances observed from 30 to 50 cm (Figure 4). AOB were split between families *Nitrosomonadaceae* (*Betaproteobacteria*) and *Nitrosococcaceae* (*Gammaproteobacteria*). *Gammaproteobacterial* AOB were more abundant than *Betaproteobacteria* AOB in the top 80 cm of the GP-STE, but from 90 to 100 cm *Betaproteobacteria* AOB were dominant. Less than 2.4% of the overall community were identified as NOB, but there were two representative NOB families including: *Nitrospinaceae* and *Nitrospiraceae* (Figure 4). *Nitrospiraceae* was dominant (>82% of NOB sequences) based on taxonomic classification of 16S sequences.

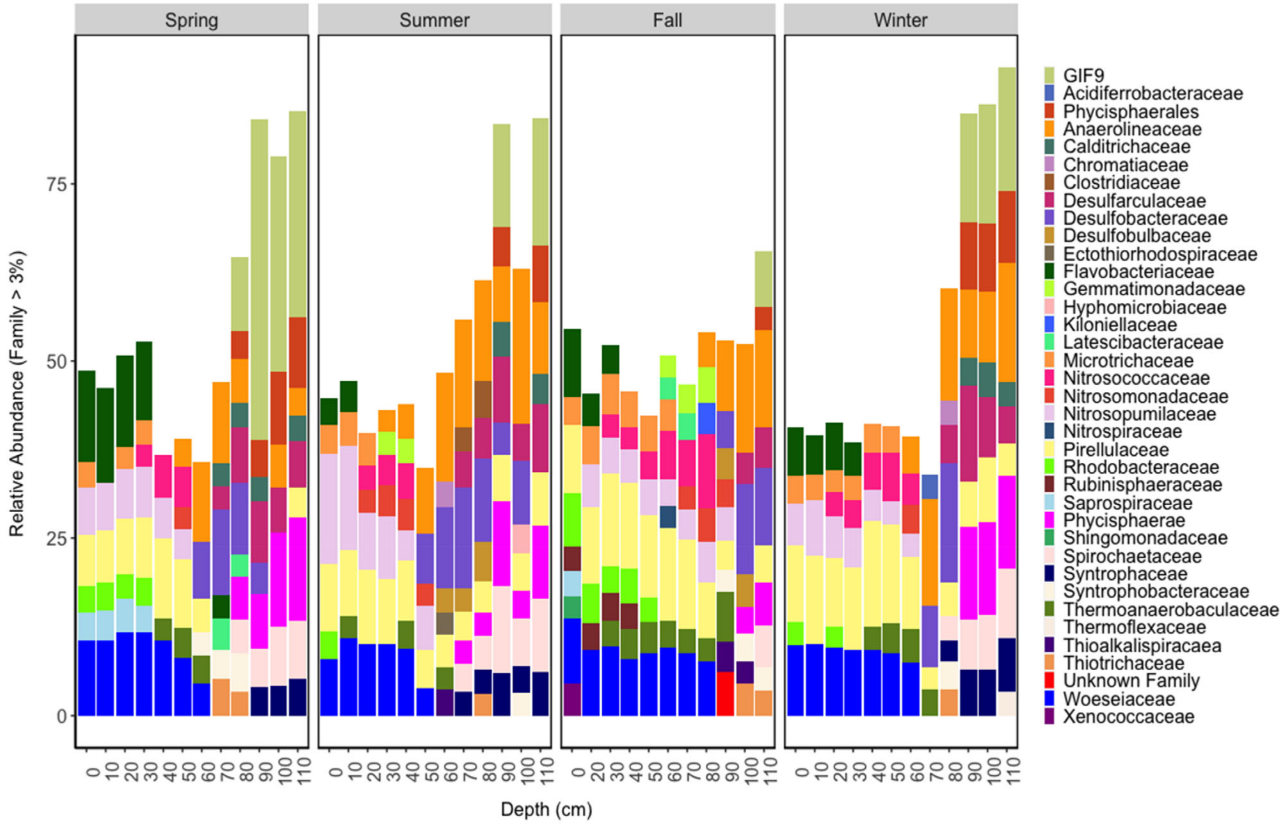

FIGURE 3 Sediment microbial community composition (family level) at each depth and season sampled at the GP-STE. Depth is labelled with the top of the respective core section depth, where 0 indicates the 0–10 cm section of the core.

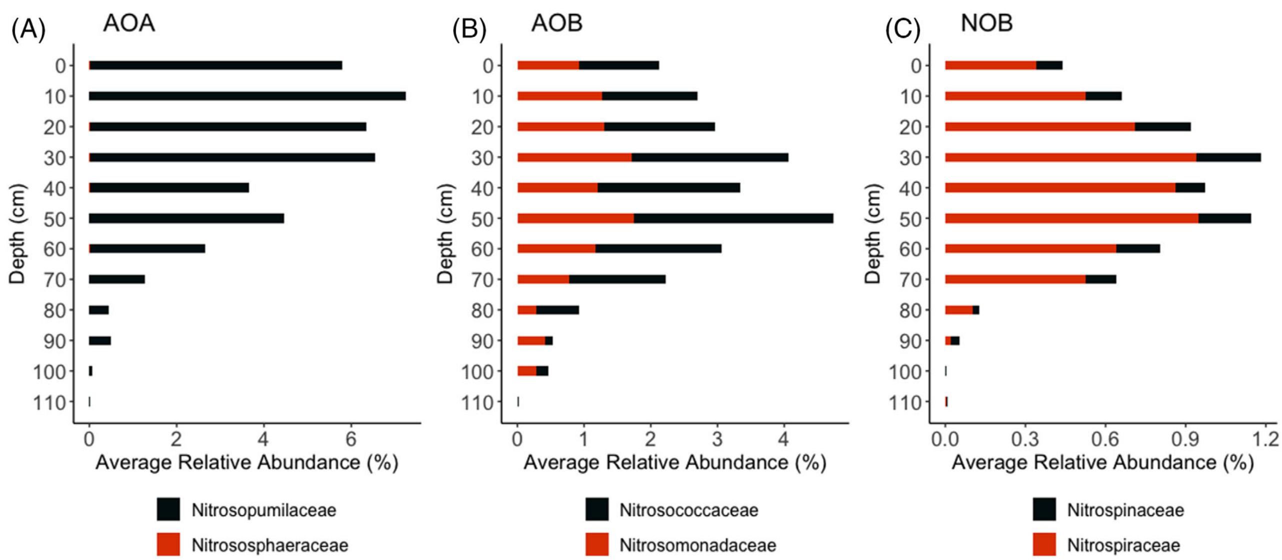

FIGURE 4 (A) AOA, (B) AOB and (C) NOB community composition shown as an average relative abundance (number of specific ASVs/total number of sample 16S ASVs × 100%) at the family level averaged across seasons sampled at each depth interval in the GP-STE. Depth is labelled by the top of the respective core section depth, where 0 indicates the top of core section 0–10 cm. AOA, ammonia oxidising archaea; AOB, ammonia oxidising bacteria; ASV, amplicon sequence variant; NOB, nitrite oxidising bacteria.

amoA gene abundances

The *amoA* genes from AOA and *Betaproteobacterial* AOB were detected and quantified with qPCR assays. The *amoA* gene abundances ranged from 1.7×10^3 to 1.9×10^5 and 6.4×10^2 to 1.16×10^5 copies g of sediment^{-1} for AOA and *Betaproteobacterial* AOB, respectively (Table S2). A one-way ANOVA confirmed

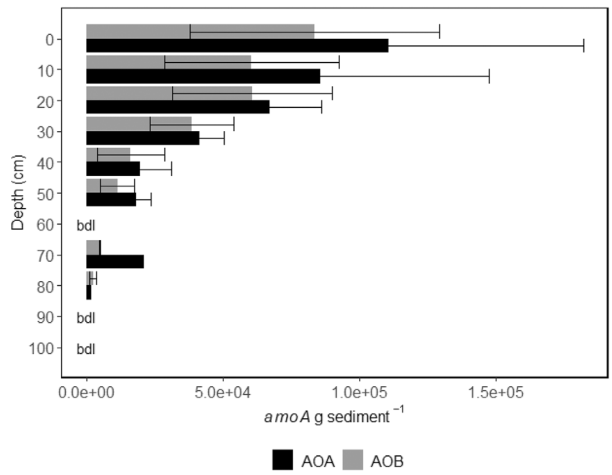

FIGURE 5 Abundance of archaeal (black) and bacterial (grey) *amoA* genes (copies g sediment^{-1}) at each sediment depth averaged across seasons sampled at the GP-STE where 0 indicates core section 0–10 cm; error bars represent one standard deviation in each direction.

there was no effect of season on *amoA* abundances (Figures S4 and S5), but the highest numbers of AOA and *Betaproteobacterial* AOB *amoA* abundances were observed in summer and the lowest abundances in winter (Figure S4). AOA and *Betaproteobacterial* AOB abundances both decreased with depth (Figure 5) and the highest abundances of ammonia oxidisers were in the top 50 cm. When averaged across sampled seasons, the number of *amoA* genes from AOA exceeds the number of *Betaproteobacterial amoA* genes at depths 0–60 cm (Figure 5). Below 60 cm the total abundance of *amoA* genes at each depth is <30 copies g^{-1} of sediment. The AOA: *Betaproteobacterial* AOB ratio ranged from 0.82 to 2.51 observed at 100 and 60 cm, respectively.

Geochemical features related to amoA abundances

qPCR quantification of AOA and *Betaproteobacterial amoA* abundances were used as response variables when comparing abundances to STE geochemical features. Explanatory variables included in the linear models were geochemical characteristics, including salinity, DO, pH, porewater DIN concentrations and extractable DIN concentrations (Tables S3 and S4). Linear regressions of AOA *amoA* abundance compared to individual STE analytes revealed significant, but weak linear relationships to porewater nitrate ($r^2 = 0.16$) and extractable nitrate ($r^2 = 0.26$) concentrations (Figure S8). *Betaproteobacterial amoA* abundances also had weak, but significant linear relationships with DO ($r^2 = 0.17$), Salinity ($r^2 = 0.13$), porewater nitrate ($r^2 = 0.21$), extractable nitrate ($r^2 = 0.33$) and extractable ammonium ($r^2 = 0.11$) concentrations (Figure S9). Both AOA ($r^2 = 0.53$) and *Betaproteobacterial* AOB ($r^2 = 0.62$) abundances had positive, linear relationships to porewater pH (Figure S7).

Hypothesis-based combinations of explanatory variables were tested to explain *amoA* abundance in a multiple linear regression analysis. Table 1 shows the top three, most parsimonious models that explained AOA and *Betaproteobacterial* AOB abundances. The model (H_{1A}) that best explained AOA abundance included porewater NO_3^-, NO_2^- and NH_4^+ concentrations, extractable NO_3^- and NH_4^+ concentrations and porewater pH (Table 1). H_{1A} explained 48% of the variation in AOA abundance (p-value $= 2.8 \times 10^{-5}$), had the lowest dAICc value (0.0), and the highest model weight (0.6). All the top three models explaining AOA abundance included nutrient concentrations (porewater and extractable) and pH, but the second and third top models also included salinity and DO, respectively. *Betaproteobacterial* AOB abundance was best explained by the model that included porewater nutrient concentrations, extractable nutrient concentrations, pH and salinity (Table 1, H_{1B}). H_{1B} explained 67% of the variation in *Betaproteobacterial* AOB abundance (p-value $= 7.7 \times 10^{-8}$) and was the most parsimonious according to dAICc (0.0) and model weight (0.5) (Table 1). H_{2B} included nutrients (porewater and extractable) and pH, but not salinity; whereas H_{3B} included nutrients, pH and DO.

DISCUSSION

Geochemical gradients along with depth in the GP-STE

The elevated concentrations of NH_4^+ and DIC co-occurring with lower pH in the deep, anoxic portion of the GP-STE are likely explained by remineralisation of organic matter along the groundwater flow-path. At the suboxic transition zone, NH_4^+ concentrations decreased as DO and NO_3^- concentrations increased (Figure 1). This could be explained by NH_4^+ transport by groundwater advection that is consumed by nitrifiers producing NO_3^-. The presence of extractable NO_3^- and lack of extractable NH_4^+ in surficial sediment could also result from nitrification. It should be noted that DIN concentrations are lower in the top four sampling depths (0–30 cm) than in the deeper porewater, this may be the result of tidal pumping, diluting DIN concentrations and flushing NO_3^- out to overlying water. Spatial and temporal variations in STE geochemical profiles are further described by Wilson et al. (2023) and similar patterns were observed at this site by Beck et al. (2016) and Hong et al. (2019).

TABLE 1 Three most parsimonious models as determined by the delta Akaike information criterion corrected (dAICc), variance explained (R^2), and model weights (Wt) for AOA and AOB abundances based on *amoA* gene quantification. H is the hypothesis number, Model includes the dependent variable (log[*amoA* copy numbers g^{-1}]) and explanatory variables (porewater NO_3, NO_2 and NH_4, extractable (EX) NO_3 and NH_4, pH, Sal = salinity and DO).

amoA	H	Model	dAICc	R^2	Wt
AOA	H_{1A}	AOA ~ NO_3 + NO_2 + NH_4 + EX(NO_3) + EX(NH_4) + pH	0	0.48	0.6
	H_{2A}	AOA ~ NO_3 + NO_2 + NH_4 + EX(NO_3) + EX(NH_4) + pH + Sal	1.6	0.49	0.3
	H_{3A}	AOA ~ NO_3 + NO_2 + NH_4 + EX(NO_3) + EX(NH_4) + pH + DO	3.2	0.47	0.1
AOB	H_{1B}	AOB ~ NO_3 + NO_2 + NH_4 + EX(NO_3) + EX(NH_4) + pH + Sal	0	0.67	0.5
	H_{2B}	AOB ~ NO_3 + NO_2 + NH_4 + EX(NO_3) + EX(NH_4) + pH	1.3	0.63	0.3
	H_{3B}	AOB ~ NO_3 + NO_2 + NH_4 + EX(NO_3) + EX(NH_4) + pH + Sal + DO	2.9	0.65	0.1

Stratification of microbial and nitrifying communities of the GP-STE

The effect of season on STE sediment microbial communities was minor when compared to community shifts observed with depth. However, the shifts that were observed with the season may be the result of seasonal shifts in hydraulic gradients. In winter and early spring at this site, vertical hydraulic gradients indicating recharge or movement of the seepage face were periodically observed (Wilson et al., 2023). This can be the result of lower rainfall during the winter months leading to lower groundwater flow or higher winter tidal heights increasing the pressure from the overlying water and decreasing groundwater flow (Moore, 1999). The small shifts in community composition observed across seasons were surprising as STEs are typically thought of as highly variable and heterogeneous systems. Our data suggest that the resident community is relatively stable seasonally. This aligns with observations of seasonally persistent gradients of salinity and oxygen with depth (Wilson et al., 2023), which were significant explanatory features for community composition in the GP-STE.

The changes in microbial community composition observed with depth (*p*-value <0.05) were tightly linked to the observed geochemical gradients of DO, salinity, DIN and DIC (Figure S2). Our results align with previous work at this site (Hong et al., 2019) and in coastal aquifers suggesting environmental factors including temperature, salinity, pH, DO, nutrient concentrations and redox conditions are related to community structure (Adyasari et al., 2019, 2020; Beck et al., 2017; Davis and Garey, 2018; McAllister et al., 2015). The families of *Nitrosococcaceae*, *Nitrosomonadaceae*, *Methyloligellaceae* and *Flavobacteriaceae* were only observed in the top 60 to 80 cm of the STE, whereas the families of *Desulfobulbaceae* and *Desulfobacteraceae*, involved in sulphur metabolism, were only present below 70 cm. *Nitrosococcaceae* and *Nitrosomonadaceae* are nitrifying organisms supporting our hypothesis that nitrification is occurring in the surficial, oxic and transition, suboxic zones of the GP-STE. A previous study conducted at this site also observed the potential for ammonia oxidation and sulphur metabolism within the microbial community (Hong et al., 2019). The resident microbial community and the cycling of nutrients and organic matter in the subsurface are critically linked, one influencing the other and, therefore, controlling exports from STE systems (Santoro et al., 2008).

The AOA community was dominated by *Nitrosopumilaceae*, a family of marine, freshwater and terrestrial ammonia oxidisers (Tolar et al., 2019). The genus classifications for AOA observed in this family (Figure S3) included *Candidatus Nitrosopumilus*, *Cenarchaeum*, *Nitrosarchaeum* and *Candidatus Nitrocosmicus*. The AOA community also included *Nitrososphaeraceae* (family), comprised of genus *Candidatus Nitrosopelagicus*, observed in the STE, which are a group of soil ammonia oxidisers (Tourna et al., 2011). The AOB communities were comprised of two families; *Nitrosomonadaceae*, which have been found in terrestrial, freshwater and marine ecosystems (Prosser et al., 2014), and *Nitrosococcaceae*, which are a group of marine *Gammaproteobacteria*. *Nitrosococcaceae* and *Nitrosomonadaceae* each represented roughly 50% of the AOB communities in the top 30 cm of the STE, whereas *Nitrosococcaceae* represented a large portion (>60%) the AOB communities from 40 to 80 cm, and from 90 to 100 cm there was a switch to *Nitrosomonadaceae* dominance (>60%).

Previous studies examining nitrifiers in STEs have focused solely on AOA and AOB, mediating the first step of nitrification (Hong et al., 2019; Santoro et al., 2008). We observed NOB in the GP-STE, including two marine NOB families, *Nitrospiraceae* and *Nitrospinaceae*. Marine *Nitrospira* are typically found in natural aquatic ecosystems in the water column or attached to sediments (Daims et al., 2015). The relative abundance of these NOB is low compared to AOA and AOB, which could suggest an imbalance in NO_2^- production and consumption by nitrification, which was hypothesised to be the case in a marine hypoxic zone (Lau et al., 2019).

The nitrifying communities (AOA, AOB and NOB) found at the GP-STE site were comprised of marine and freshwater taxa suggesting a consortium that may be derived from both groundwater and overlying seawater. There was little variation in nitrifier community structure with depth, which was unexpected as depth had a significant impact on the larger microbial community structure. Salinity has been shown to cause shifts in ammonia oxidiser community composition (Bernhard et al., 2005; Biller et al., 2012; Mosier & Francis, 2008; Rogers & Casciotti, 2010; Santoro et al., 2008), but our data do not suggest salinity influences ammonia oxidiser community (family level) in the GP-STE. DO concentrations (Geets et al., 2006) have also been related to AOB community composition; however, variation in AOB community composition (family level) in our study did not change with porewater DO.

Geochemical features related to amoA gene abundances in the GP-STE

AOA and *Betaproteobacterial* AOB abundances were weakly explained by DO, Salinity, porewater nitrate, extractable nitrate and extractable ammonium (Figures S8 and S9). This aligned with the multiple linear regression analysis, that suggested geochemical factors including the same variables (DIN concentrations, pH, DO and salinity) are important explanatory variables for AOA and *Betaproteobacterial* AOB abundances. The multiple linear regressions had higher explanatory power for abundance than any individual linear regression, except for pH. Previous work on *amoA* gene abundances have found that AOA or *Betaproteobacterial* AOB distributions were explained by sediment conditions observed with depth, such as nutrient limitation, in subsurface floodplain soils (Cardarelli et al., 2020). Substrate availability was also hypothesised to explain shifts in *amoA* gene abundances observed seasonally in estuarine sediments (Lisa et al., 2015). Similarly, extractable and porewater DIN concentrations were included in all the most parsimonious models for AOA and *Betaproteobacterial* AOB; confirming that substrate availability and or limitation is likely important to nitrifier abundance (Bouskill et al., 2012; Caffrey et al., 2007).

Porewater pH was an important explanatory variable for AOA and *Betaproteobacterial* AOB abundances in the GP-STE. There was a positive, linear relationship between pH and ammonia oxidiser abundance (Figure S7), with lower abundance at lower pH values. The availability of NH_3 decreases as pH decreases and, subsequently, ammonia oxidation rates also decrease (Beman et al., 2011; Wannicke et al., 2018). This relationship may have biogeochemical implications as ocean acidification (OA) lowers the pH of marine systems. The unique mixing in STEs of seawater with groundwater, which typically has a lower pH compared to seawater, can give insight to how nitrifying communities may respond to decreases in pH. Previous work reports nitrification may be suppressed following lowered pH due to OA (Beman et al., 2011; Pajares & Ramos, 2019; Wannicke et al., 2018), our data suggest that pH may also influence nitrifier abundance in sandy sediments.

Porewater salinity was included in the most parsimonious model (H_{1B}) for *Betaproteobacterial* AOB, but not AOA (H_{1A}). This could indicate that *Betaproteobacterial* AOB have a greater sensitivity to salinity than AOA. Interestingly, DO was not in the most parsimonious model for either AOA or *Betaproteobacterial* AOB. Active AOA have been observed in oxygen minimum zones and in cultures with low micromolar levels of DO (Qin et al., 2017) and, therefore, may be more resilient to changes in DO, making substrate availability and pH more important in determining their distribution. Deoxygenation in marine and coastal ecosystems is projected to increase with climate change (Levin & Breitburg, 2015); these conditions could lead to lower nitrification rates and decreased nitrifier abundance.

Salinity has also been shown to effect both AOA and *Betaproteobacterial* AOB abundances in STEs (Santoro et al., 2008), surface estuaries (Mosier & Francis, 2008) and salt marsh sediments (Moin et al., 2009). Our results indicate that salinity is important, specifically to *Betaproteobacterial* AOB abundance, but other geochemical factors such as pH, and nutrient concentrations, may be more significant to determining AOA abundances in the subsurface.

CONCLUSIONS

In this study we examined microbial community structure and, more specifically, the nitrifying community of a sandy sediment STE across depth and seasons. Microbial community structure followed the distinct stratification of observed geochemical gradients with depth but was largely stable across seasons. AOA, AOB and NOB were present, suggesting both ammonia and nitrite oxidation could occur in the STE. Due to the variable nature of these systems, we were able to assess if geochemical factors influence nitrification in the subsurface. Our data support previous work suggesting substrates, salinity and DO are important explanatory variables for ammonia oxidiser abundance. We also found that pH plays a significant role in determining both AOA and *Betaproteobacterial* AOB abundances, which could have implications for nitrification in the face of OA. This study contributes to our understanding of the microbial dimension of STEs, suggesting that community composition shifts with depth, which aligns with STE geochemical gradients, and outweighs the impact of seasonality. This has important implications for how we understand resident microbial communities and biogeochemical functions in STEs over time and space.

The influence of biogeochemistry and specific condition on microbial communities and nitrogen cycling microorganisms can help us better understand critical geochemical fluxes from groundwater in coastal environments.

AUTHOR CONTRIBUTIONS

Stephanie J. Wilson: Conceptualization (equal); investigation (lead); data curation and analysis (lead); writing (lead). **Bongkeun Song:** Conceptualization (equal); resources (equal); investigatin (supporting); writing – review and editing (equal). **Iris C. Anderson:** Conceptualization (equal); resources (equal); writing – review and editing (equal).

ACKNOWLEDGEMENTS

This project was funded by the National Science Foundation (1658135 and 1737258) and the Virginia Institute of Marine Science. We thank Dr. Chris Hein and Jennifer Connell for their help with sediment core collection. We also thank Michele Cochran and Hunter Walker for aid in sample collection and analytical procedures. Lastly, we thank Renia Prassie and Gail Scott for help with molecular analyses and Illumina MiSeq maintenance. The graphical abstract was created using Biorender (https://www.biorender.com/).

CONFLICT OF INTEREST STATEMENT

The authors declare no conflict of interest.

DATA AVAILABILITY STATEMENT

Geochemical gradient data are available via BCO DMO at DOI: 10.26008/1912/bco-dmo.807664.1 (https://www.bco-dmo.org/dataset/807664/data). 16S sequences referenced in this work are available via NCBI with accession number: PRJNA804121 (https://www.ncbi.nlm.nih.gov/bioproject/PRJNA804121/).

ORCID

Stephanie J. Wilson https://orcid.org/0000-0002-5484-0748
Bongkeun Song https://orcid.org/0000-0002-6645-7025
Iris C. Anderson https://orcid.org/0000-0001-5879-6038

REFERENCES

Adyasari, D., Oehler, T., Afiati, N. & Moosdorf, N. (2019) Environmental impact of nutrient fluxes associated with submarine groundwater discharge at an urbanized tropical coast. *Estuarine, Coastal and Shelf Science*, 221, 30–38.

Adyasari, D., Hassenruck, C., Montiel, D. & Dimova, N. (2020) Microbial community composition across a coastal hydrological system affected by submarine groundwater discharge (SGD). *PLoS One*, 15, 1–16.

Anschutz, P., Charbonnier, C., Deborde, J., Deirmendjian, L., Poirier, D., Mouret, A. et al. (2016) Terrestrial groundwater and nutrient discharge along the 240-km-long Aquitanian coast. *Marine Chemistry*, 185, 38–47.

Beck, A.J., Kellum, A.A., Luek, J.L. & Cochran, M.A. (2016) Chemical flux associated with spatially and temporally variable submarine groundwater discharge, and chemical modification in the subterranean estuary at Gloucester point, VA (USA). *Estuaries and Coasts*, 39, 1–12.

Beck, M., Reckhardt, A., Amelsberg, J., Bartholomä, A., Brumsack, H.J., Cypionka, H. et al. (2017) The drivers of biogeochemistry in beach ecosystems: a cross-shore transect from the dunes to the low-water line. *Marine Chemistry*, 190, 35–50.

Beman, J.M., Chow, C.E., King, A.L., Feng, Y., Fuhrman, J.A., Andersson, A. et al. (2011) Global declines in oceanic nitrification rates as a consequence of ocean acidification. *Proceedings of the National Academy of Sciences of the United States of America*, 108, 208–213.

Bernhard, A.E., Donn, T., Giblin, A.E. & Stahl, D.A. (2005) Loss of diversity of ammonia-oxidizing bacteria correlates with increasing salinity in an estuary system. *Environmental Microbiology*, 7, 1289–1297.

Biller, S.J., Mosier, A.C., Wells, G.F. & Francis, C.A. (2012) Global biodiversity of aquatic ammonia-oxidizing archaea: is partitioned by habitat. *Frontiers in Microbiology*, 3, 1–15.

Bouskill, N.J., Eveillard, D., Chien, D., Jayakumar, A. & Ward, B.B. (2012) Environmental factors determining ammonia-oxidizing organism distribution and diversity in marine environments. *Environmental Microbiology*, 14, 714–729.

Caffrey, J.M., Bano, N., Kalanetra, K. & Hollibaugh, J.T. (2007) Ammonia oxidation and ammonia-oxidizing bacteria and archaea from estuaries with differing histories of hypoxia. *ISME Journal*, 1, 660–662.

Callahan, B.J., McMurdie, P.J., Rosen, M.J., Han, A.W., Johnson, A.J.A. & Holmes, S.P. (2016) DADA2: high-resolution sample inference from Illumina amplicon data. *Nature Methods*, 13, 581–583.

Caporaso, J.G., Lauber, C.L., Walters, W.A., Berg-Lyons, D., Huntley, J., Fierer, N. et al. (2012) Ultra-high-throughput microbial community analysis on the Illumina HiSeq and MiSeq platforms. *ISME Journal*, 6, 1621–1624.

Cardarelli, E.L., Bargar, J.R. & Francis, C.A. (2020) Diverse Thaumarchaeota dominate subsurface ammonia-oxidizing communities in semi-arid floodplains in the Western United States. *Microbial Ecology*, 80, 778–792.

Charette, M.A., Allen, M.C. & Sites, F. (2006) Precision ground water sampling in coastal aquifers using a direct-push, shielded-screen well-point system. *Groundwater Monitoring and Remediation*, 26, 87–93.

Couturier, M., Tommi-Morin, G., Sirois, M., Rao, A., Nozais, C. & Chaillou, G. (2017) Nitrogen transformations along a shallow subterranean estuary. *Biogeosciences*, 14, 3321–3336.

Daims, H., Lebedeva, E.V., Pjevac, P., Han, P., Herbold, C., Albertsen, M. et al. (2015) Complete nitrification by Nitrospira bacteria. *Nature*, 528, 504–509.

Davis, M.C. & Garey, J.R. (2018) Microbial function and hydrochemistry within a stratified anchialine sinkhole: a window into coastal aquifer interactions. *Water*, 10, 1–17. Available from: https://doi.org/10.3390/w10080972

Erler, D.V., Santos, I.R., Zhang, Y., Tait, D.R., Befus, K.M., Hidden, A. et al. (2014) Nitrogen transformations within a tropical subterranean estuary. *Marine Chemistry*, 164, 38–47.

Fox, J., Weisberg, S., Price, B., Adler, D., Bates, D., Baud-Bovy, G. et al. (2019) Car: companion to applied regression. R Package Version 3.0-2.

Francis, C.A., Roberts, K.J., Beman, J.M., Santoro, A.E. & Oakley, B.B. (2005) Ubiquity and diversity of ammonia-oxidizing archaea in water columns and sediments of the ocean. *Proceedings of the National Academy of Sciences of the United States of America*, 102, 14683–14688.

Geets, J., Boon, N. & Verstraete, W. (2006) Strategies of aerobic ammonia-oxidizing bacteria for coping with nutrient and oxygen fluctuations. *FEMS Microbiology Ecology*, 58, 1–13.

Graham, E.B., Knelman, J.E., Schindlbacher, A., Siciliano, S., Breulmann, M., Yannarell, A. et al. (2016) Microbes as engines of ecosystem function: when does community structure enhance predictions of ecosystem processes? *Frontiers in Microbiology*, 7, 1–10.

Hong, Y., Wu, J., Wilson, S. & Song, B. (2019) Vertical stratification of sediment microbial communities along geochemical gradients of a subterranean estuary located at the Gloucester Beach of Virginia, United States. *Frontiers in Microbiology*, 9, 1–11.

Hug, L.A., Thomas, B.C., Sharon, I., Brown, C.T., Sharma, R., Hettich, R.L. et al. (2016) Critical biogeochemical functions in the subsurface are associated with bacteria from new phyla and little studied lineages. *Environmental Microbiology*, 18, 159–173. Available from: https://doi.org/10.1111/1462-2920.12930

Lau, E., Frame, C.H., Nolan, E.J., IV, Stewart, F.J., Dillard, Z.W., Lukich, D.P. et al. (2019) Diversity and relative abundance of ammonia- and nitrite-oxidizing microorganisms in the offshore Namibian hypoxic zone. *PLoS One*, 14, 1–20. Available from: https://doi.org/10.1371/journal.pone.0217136

Levin, L.A. & Breitburg, D.L. (2015) Linking coasts and seas to address ocean deoxygenation. *Nature Climate Change*, 5, 401–403.

Lisa, J.A., Song, B., Tobias, C.R. & Hines, D.E. (2015) Genetic and biogeochemical investigation of sedimentary nitrogen cycling communities responding to tidal and seasonal dynamics in Cape Fear River Estuary. *Estuarine, Coastal and Shelf Science*, 167, A313–A323.

McAllister, S.M., Barnett, J.M., Heiss, J.W., Findlay, A.J., MacDonald, D.J., Dow, C.L. et al. (2015) Dynamic hydrologic and biogeochemical processes drive microbially enhanced iron and sulfur cycling within the intertidal mixing zone of a beach aquifer. *Limnology and Oceanography*, 60, 329–345. Available from: https://doi.org/10.1002/lno.10029

McLachlan, A. & Brown, A.C. (2006) *The ecology of sandy shores*. Burlington: Academic Press.

McMurdie, P.J. & Holmes, S. (2013) Phyloseq: an R package for reproducible interactive analysis and graphics of microbiome census data. *PLoS One*, 8, e61217.

Moore, W.S. (1999) The subterranean estuary: a reaction zone of ground water and sea water. *Marine Chemistry*, 65, 111–125.

Moin, N.S., Nelson, K.A., Bush, A. & Bernhard, A.E. (2009) Distribution and diversity of archaeal and bacterial ammonia oxidizers in salt marsh sediments. *Applied and Environmental Microbiology*, 75, 7461–7468. Available from: https://doi.org/10.1128/AEM.01001-09

Mosier, A.C. & Francis, C.A. (2008) Relative abundance and diversity of ammonia-oxidizing archaea and bacteria in the San Francisco Bay estuary. *Environmental Microbiology*, 10, 3002–3016.

Norton, J.M., Alzerreca, J.J., Suwa, Y. & Klotz, M.G. (2002) Diversity of ammonia monooxygenase operon in autotrophic ammonia-oxidizing bacteria. *Archives of Microbiology*, 177, 139–149.

Okano, Y., Hristova, K.R., Leutenegger, C.M., Jackson, L.E., Denison, R.F., Gebreyesus, B. et al. (2004) Application of real-time PCR to study effects of ammonium on population size of ammonia-oxidizing bacteria in soil. *Applied and Environmental Microbiology*, 70, 1008–1016.

Oksanaen, J.,.F., Blanchet, G. & Friendly, M. (2019) Vegan: community ecology package. R package version 2.5-6.

Pajares, S. & Ramos, R. (2019) Processes and microorganisms involved in the marine nitrogen cycle: knowledge and gaps. *Frontiers in Marine Science*, 6, 1–33.

Parada, A.E., Needham, D.M. & Fuhrman, J.A. (2015) Every base matters: assessing small subunit rRNA primers for marine microbiomes with mock communities, time series and global field samples. *Environmental Microbiology*, 18, 1403–1414.

Pjevac, P., Schauberger, C., Poghosyan, L., Herbold, C.W., van Kessel, M.A.H.J., Daebeler, A. et al. (2017) AmoA-targeted polymerase chain reaction primers for the specific detection and quantification of comammox Nitrospira in the environment. *Frontiers in Microbiology*, 8, 1–11.

Prosser, J.I., Head, I.M. & Stein, L.Y. (2014) The family Nitrosomonadaceae. In: Rosenberg, E., DeLong, E.F., Lory, S., Stackebrandt, E. & Thompson, F. (Eds.) *The Prokaryotes: Alphaproteobacteria and Betaproteobacteria*. Berlin, Heidelberg: Springer Berlin Heidelberg, pp. 901–918.

Prosser, J.I. & Nicol, G.W. (2008) Relative contributions of archaea and bacteria to aerobic ammonia oxidation in the environment. *Environmental Microbiology*, 10, 2931–2941.

Qin, S., Pang, Y., Clough, T., Wrage-Mönnig, N., Hu, C., Zhang, Y. et al. (2017) N_2 production via aerobic pathways may play a significant role in nitrogen cycling in upland soils. *Soil Biology and Biochemistry*, 108, 36–40.

Qin, W., Martens-Habbena, W., Kobelt, J.N. & Stahl, D.A. (2016) *Candidatus Nitrosopumilus*. *Bergey's Manual of Systematics of Archaea and Bacteria*, 1–9.

Quast, C., Pruesse, E., Yilmaz, P., Gerken, J., Schweer, T., Yarza, P. et al. (2013) The SILVA ribosomal RNA gene database project: improved data processing and web-based tools. *Nucleic Acids Research*, 41, 590–596.

Reed, D.W., Smith, J.M., Francis, C.A. & Fujita, Y. (2010) Responses of ammonia-oxidizing bacterial and archaeal populations to organic nitrogen amendments in low-nutrient groundwater. *Applied and Environmental Microbiology*, 76, 2517–2523.

Rogers, D.R. & Casciotti, K.L. (2010) Abundance and diversity of archaeal ammonia oxidizers in a coastal groundwater system. *Applied and Environmental Microbiology*, 76, 7938–7948.

Rotthauwe, J.-H., Witzel, K.-P. & Liesack, W. (1997) The ammonia monooxygenase structural gene amoA as a functional marker: molecular fine-scale analysis of natural ammonia-oxidizing populations. *Applied and Environmental Microbiology*, 63, 4704–4712.

Ruiz-González, C., Rodellas, V. & Garcia-Orellana, J. (2021) The microbial dimension of submarine groundwater discharge: current challenges and future directions. *FEMS Microbiology Reviews*, 45, 1–25.

Santoro, A.E. (2010) Microbial nitrogen cycling at the saltwater—freshwater interface. *Hydrogeology Journal*, 18, 187–202.

Santoro, A.E. (2016) The do-it-all nitrifier. *Science*, 351, 342–343.

Santoro, A.E., Francis, C.A., De Sieyes, N.R. & Boehm, A.B. (2008) Shifts in the relative abundance of ammonia-oxidizing bacteria and archaea across physicochemical gradients in a subterranean estuary. *Environmental Microbiology*, 10, 1068–1079.

Santos, I.R., Burnett, W.C., Chanton, J., Mwashote, B., Suryaputra, I.G.N.A. & Dittmar, T. (2008) Nutrient biogeochemistry in a Gulf of Mexico subterranean estuary and groundwater-derived fluxes to the coastal ocean. *Limnology and Oceanography*, 53, 705–718.

Seitzinger, S., Harrison, J.A., Bohlke, J.K., Bouwman, A.F., Lowrance, R., Peterson, B. et al. (2006) Denitrification across landscapes and waterscapes: a synthesis. *Ecological Applications*, 16, 2064–2090.

Slomp, C.P. & Van Cappellen, P. (2004) Nutrient inputs to the coastal ocean through submarine groundwater discharge: controls and potential impact. *Journal of Hydrology*, 295, 64–86.

Thompson, L., Sanders, J., McDonald, D., Amir, A., Ladau, J., Locey, K.J. et al. (2017) A communal catalogue reveals Earth's multiscale microbial diversity. *Nature*, 551, 457–463.

Tolar, B.B., Mosier, A.C., Lund, M.B. & Francis, C.A. (2019) Nitrosarchaeum. In: *Bergey's Manual of Systematics of Archaea and Bacteria*. John Wiley & Sons, Inc. Available from: https://doi.org/10.1002/9781118960608.gbm01289

Tourna, M., Stieglmeier, M., Spang, A., Könneke, M., Schintlmeister, A., Urich, T. et al. (2011) *Nitrososphaera viennensis*, an ammonia oxidizing archaeon from soil. *Proceedings of the National Academy of Sciences of the United States of America*, 108, 8420–8425.

van Kessel, M.A.H.J., Speth, D.R., Albertsen, M., Nielsen, P.H., Op den Camp, H.J.M., Kartal, B. et al. (2015) Complete nitrification by a single microorganism. *Nature*, 528, 555–559.

Wannicke, N., Frey, C., Law, C.S. & Voss, M. (2018) The response of the marine nitrogen cycle to ocean acidification. *Global Change Biology*, 24, 5031–5043.

Wilson, S.J., Anderson, I.C., Song, B. & Tobias, C.R. (2023) Temporal and spatial variations in subterranean estuary geochemical gradients and nutrient cycling rates: impacts on groundwater nutrient export to estuaries. *Journal of Geophysical Research – Biogeosciences*, 128, 1–19.

Wu, J., Hong, Y., Wilson, S.J. & Song, B. (2021) Microbial nitrogen loss by coupled nitrification to denitrification and anammox in a permeable subterranean estuary at Gloucester Point, Virginia. *Marine Pollution Bulletin*, 168, 1–10.

SUPPORTING INFORMATION

Additional supporting information can be found online in the Supporting Information section at the end of this article.

How to cite this article: Wilson, S.J., Song, B. & Anderson, I.C. (2023) Geochemical factors impacting nitrifying communities in sandy sediments. *Environmental Microbiology*, 1–12. Available from: https://doi.org/10.1111/1462-2920.16504